IOPscience iopscience.iop.org

Home Search Collections Journals About Contact us My IOPscience

Conductivity and magnetoresistance of hydrogenated amorphous silicon-nickel alloys near the metal-insulator transition

This article has been downloaded from IOPscience. Please scroll down to see the full text article.

1992 J. Phys.: Condens. Matter 4 9113

(http://iopscience.iop.org/0953-8984/4/46/017)

View the table of contents for this issue, or go to the journal homepage for more

Download details:
IP Address: 171.66.16.96
The article was downloaded on 11/05/2010 at 00:53

Please note that terms and conditions apply.

J. Phys.: Condens. Matter 4 (1992) 9113–9130. Printed in the UK

Conductivity and magnetoresistance of hydrogenated amorphous silicon–nickel alloys near the metal–insulator transition

K M Abkemeier†, C J Adkins†, R Asal‡ and E A Davis‡

† Cavendish Laboratory, Madingley Road, Cambridge CB3 0HE, UK

‡ Department of Physics and Astronomy, University of Leicester, Leicester LE1 7RH, UK

Received 19 May 1992, in final form 24 July 1992

Abstract. We present conductivity and magnetoresistance data for a range of a-$Si_{1-y}Ni_y$:H alloys near the metal–insulator transition. In the metallic regime, weak-localization and interaction effects are identified, the latter being of normal sign. In the activated regime, conductivity results imply variable-range hopping in a parabolic density of states, but quantitative analysis shows that if this density of states results from a Coulomb gap, then the localized states extend over large clusters of nickel atoms. The magnetoresistance data generally show positive magnetoresistance attributed to spin splitting in interaction effects, but negative magnetoresistance, attributed to suppression of weak-localization-type interference, is seen on the insulating side of the transition at not too low temperatures where interaction effects are partially suppressed.

1. Introduction

The metal–insulator transition in amorphous metal–semiconductor alloys has been an active field experimentally over recent years, with alloys of silicon and germanium having been investigated in particular. The interest in these systems arises because the metals used form deep donor states in the host semiconductor. In such cases, the metal–insulator transition is less studied and not nearly as well understood as that in systems involving shallow donor or acceptor states such as occur in crystalline silicon doped with phosphorus or arsenic. The stronger binding to the metal atoms means that much higher concentrations are needed to reach the transition to the metallic state and percolation aspects are more likely to be of importance. Additionally, there has recently been particular interest in systems in which the metal is magnetic because some studies have given evidence of a reversal of sign of the long-range electron–electron interaction contribution to the conductivity. These considerations led to the present study a-$Si_{1-y}Ni_y$:H. In this paper, we present conductivity and magnetoresistance data and discuss our results in the context of the current understanding of metal–insulator transitions in systems of this kind.

2. Current theoretical context

Experimental results on conductivity in disordered systems near the metal–insulator transition have to be discussed in terms of current theoretical ideas. In this section,

0953-8984/92/469113+18$07.50 © 1992 IOP Publishing Ltd

we give a brief description of the key concepts involved in current models. Reviews have been given by Lee and Ramakrishnan (1985) and, more recently, by Mott (1990). The following account refers entirely to three-dimensional systems.

2.1. Nature of the metal–insulator transition

According to simple theory, conductivity σ of *metallic systems* may be expressed

$$\sigma_B = ne^2\tau/m = ne^2\ell/mv_F \tag{1}$$

where n is the number density of the carriers having charge e and mass m. The time between collisions τ is determined by the various scattering processes present whose rates add to give a total scattering rate τ^{-1}. The second expression gives σ in terms of the mean free path ℓ and the Fermi velocity v_F. This is known as the *Boltzmann conductivity*.

Using free-electron theory to substitute for n, the Boltzmann conductivity may be written

$$\sigma_B = \frac{1}{3\pi^2}\frac{e^2}{\hbar}k_F^2\ell \approx \frac{1}{3\pi^2}\frac{e^2}{\hbar}\frac{\ell}{a^2} \tag{2}$$

where a is a microscopic scale length of order k_F^{-1}. Ioffe and Regel (1960) argued that increasing disorder could not cause ℓ to become less than a and, on this basis, Mott (1967) predicted a minimum metallic conductivity of order $\sigma_{min} \approx 0.03e^2/\hbar a$ (in three dimensions). In fact, σ_{min} marks the limit of validity of simplistic models of conduction and does not imply that there would be, at zero temperature, a discontinuous drop of conductivity to the insulating state at that degree of disorder. The absence of any discontinuity is supported by the arguments of *scaling theory*.

Scaling theory (see Lee and Ramakrishnan 1985) considers the way in which the conductance of a system depends on its size L. It examines the quantal nature of the conduction process and shows that the mechanisms determining the resistance of a system are consistent with continuity of resistance between metallic and insulating states. In three dimensions, the transition corresponds to the conductance on a characteristic microscopic length scale passing through a (finite) critical value g_3. An important result of the scaling analysis is that it shows that characteristic scale lengths exist on both sides of the transition. On the metallic side, the scale length is known as the *correlation length* ξ which is defined by $\sigma = g_3/\xi$. Clearly, ξ diverges at the transition since σ goes continuously to zero. On the insulating side, the conductance of a sufficiently large sample decreases exponentially with size, $g(L) = g_3\exp(-L/\xi_{loc})$ which defines the localization length ξ_{loc}. Again, ξ_{loc} diverges at the transition. Clearly, to exhibit 'bulk', ohmic behaviour, samples must be larger than the relevant scale length: $L \gg \xi$ or ξ_{loc}.

2.2. Weak localization

The Boltzmann result is only correct to first order in $1/k_F\ell$. As disorder increases, higher-order scatterings have to be taken into account and these result in a conductivity reduced below the Boltzmann value. In three dimensions (Lee and Ramakrishnan 1985)

$$\sigma = \sigma_B - \frac{e^2}{\pi^3\hbar}\left[\frac{1}{a} - \frac{1}{L}\right] \tag{3}$$

in which the system size appears in the final term. The reduction in conductivity results from constructive interference between the various multiple-scattering paths, and, remembering that in the limit of large disorder $\ell \to a$ so that $\sigma_B \to e^2/3\pi^2\hbar a$ (equation (2)), we see that the coherent scattering reduces the conductivity towards zero. It is the same scattering that eventually brings about localization. This correction to Boltzmann conductivity is called *weak localization* and it was first discussed by Bergmann (1983, 1984).

The above description applies to zero temperature. At finite temperatures, the coherence of the back scattering in weak localization is reduced if an inelastic event occurs in one of the interfering paths that contribute to the total scattering amplitude. Weak-localization effects are therefore reduced by increasing temperature and conductivity will increase. A new length scale enters the problem, the inelastic diffusion length L_i which replaces the sample size in equation (3). Since, near the metal–insulator transition, motion is diffusive, $L_i = (D\tau_i)^{1/2}$ where D is the diffusion constant and τ_i the inelastic scattering time. The form of the resulting temperature dependence depends on the origin of the inelastic event (Mott 1990). If it is by phonons or magnons at high temperature ($T > \Theta_D$ or Θ_N) the scattering rate is proportional to temperature and $\Delta\sigma \propto T^{1/2}$. For phonons, this dependence would be restricted to relatively high temperatures which would be outside the range of most experiments, but Néel temperatures can be low so that $T^{1/2}$ behaviour is possible by this mechanism in magnetically active systems at low temperatures. Phonon or magnon scattering at low temperatures ($T < \Theta_D$ or Θ_N) gives a different temperature dependence because of the changing phonon (magnon) spectrum and the varying matrix element. Mott (1990) deduces a T^4 dependence for the scattering rate and therefore a T^2 dependence for the change in conductivity. (See also section 4.1.) Finally, if the inelastic event is due to inelastic electron–electron (Landau–Baber) scattering, which alone gives a resistivity contribution varying as T^2, then its effect on weak localization gives $\Delta\sigma \sim T$.

In general, therefore, we may expect a conductivity increasing with temperature as

$$\Delta\sigma = \frac{e^2}{\hbar}\frac{1}{\pi^3 a}\left(\frac{T}{T_{wl}}\right)^{p/2} \tag{4}$$

where T_{wl} is a constant containing the details of the probability of the inelastic event which is taken to have a temperature dependence of T^p. This will only apply for $T \ll T_{wl}$ since $T = T_{wl}$ in (4) marks complete removal of weak-localization contributions to resistance.

Given the forms of the various temperature dependencies mentioned above, the dominant inelastic mechanism at low temperatures is expected to be electron–electron scattering leading to $\Delta\sigma \sim T$.

The constructive interference responsible for weak-localization effects can also be destroyed by application of a magnetic field. The partial amplitudes will be randomly dephased when approximately one flux quantum passes through the projected area of contributing paths. One defines a corresponding magnetic length $L_B = (\hbar/eB)^{1/2}$ which acts like L_i in reducing the long-range cut-off in (3). This gives rise to negative magnetoresistance which is predicted to behave as B^2 in very small fields and going over to a $B^{1/2}$ dependence at high fields (Kawabata 1980a, b).

In the above discussion it has been assumed that the interference giving rise to the coherent back-scattering is initially constructive, thus leading to decrease of resistance

with increase of temperature and, correspondingly, to negative magnetoresistance. However, some systems (e.g. palladium–carbon mixtures) appear to show weak-localization effects of reverse sign (Carl *et al* 1989) and it has been suggested that this can be explained by the presence of strong spin–orbit interaction which, it is argued, causes the initial interference to be destructive so that inelastic events increase constructive interference and reduce resistance. Such a possibility is termed *weak antilocalization*.

2.3. Electron–electron interactions

It was Altshuler and Aronov (1979) who first showed that long-range Coulomb interactions between carriers produce an anomaly in the density of states at the Fermi level. The anomaly, which takes the form of a square-root singularity dip, arises through inhibition of charge diffusion so that its strength increases with increasing disorder. Clearly, a reduced conductivity is predicted and the anomaly will become less important as temperature is raised so that the conductivity will rise with increasing temperature. A full treatment, however, has to include both Hartree and exchange terms (see Lee and Ramakrishnan 1985). The predicted form of the temperature dependence is then

$$\Delta\sigma = \frac{e^2}{\hbar}\frac{1}{4\pi^2}\frac{1.3}{\sqrt{2}}\left(\frac{4}{3}-\frac{2}{3}\tilde{F}_\sigma\right)\sqrt{\frac{kT}{\hbar D}} \tag{5}$$

where $\tilde{F}_\sigma$ is related to screening. The effect can now be of either sign depending on the relative size of the exchange and Hartree terms. The predicted $T^{1/2}$ behaviour is expected to change to $T^{1/3}$ very close to the transition (Altshuler and Aronov 1985).

The electron–electron interactions give rise to positive magnetoresistance as a result of spin splitting of certain terms involved. The change in conductivity is of the form

$$\Delta\sigma = -\frac{e^2}{\hbar}\frac{\tilde{F}_\sigma}{4\pi^2}\sqrt{\frac{kT}{2\hbar D}}g_3(h) \tag{6}$$

where $h = g\mu_B B/kT$ and g_3 again takes limiting forms varying as B^2 at low fields and as $B^{1/2}$ at high fields. A further contribution to the positive magnetoresistance comes in when the Landau orbit size becomes comparable to the 'thermal length', $(D/kT)^{1/2}$. Far from the transition, where D is large, this can become important at lower fields than the spin–orbit mechanism.

2.4. Fitting data in the metallic regime

We initially fitted our experimental results for the temperature dependence of the conductivity in the metallic regime to the form

$$\sigma = \sigma(0) + aT^{1/2} + bT^{p/2} \tag{7}$$

where the first of the temperature-dependent terms is the expected form for interaction effects and the second that for weak localization. However, in later analyses, we explored variation of both temperature indices (see section 4.1). A change in sign of the fitted $\sigma(0)$ can be taken as an indication of the position of the metal–insulator transition.

2.5. Conductivity on the insulating side of the transition

The situation on the insulating side of the metal–insulator transition is simpler. Here, conductivity is necessarily activated, and results are usually interpreted in terms of variable-range hopping of carriers between localized states. In three dimensions, the predicted form for the conductivity is

$$\sigma = \sigma_0 \exp\left[-(T_0/T)^x\right] \tag{8}$$

in which $x = (p+1)/(p+4)$ where p is the power by which the density of states $g(\epsilon)$ rises about the Fermi level as a function of energy ϵ: $g(\epsilon) = g_p|\epsilon|^p$. In a constant density of states this gives the classic Mott $T^{1/4}$ law. However, many systems, both two- and three-dimensional, show $x = 0.5$ which corresponds to variable-range hopping in a density of states of the form predicted by Efros and Shklovskii (1975) to result from Coulomb interactions between the localized carriers. In three dimensions, the corresponding density of states (for single-particle excitations) is parabolic about the Fermi level. At high temperatures, activation to extended states above the mobility edge is possible, resulting in $x \to 1$, and at intermediate temperatures, such that hopping involves states beyond the range of the Coulomb anomaly, Mott hopping can occur with $x = 0.25$.

In the hopping regime, the most obvious effect of a magnetic field is shrinking of the localized orbitals, leading to positive magnetoresistance at high magnetic fields (Yafet *et al* 1956, Shklovskii and Efros 1984). However, negative magnetoresistance is sometimes seen at low fields and two explanations have been suggested for this. The first is based on a model that invokes weak-localization-type interference between the various scattering paths involved in hopping transitions (Nguyen *et al* 1985). It is argued that the forward tunnelling amplitude is enhanced by the magnetic-field-induced phase changes in the electron wavefunctions. The second explanation is based on a model in which the shrinking of the localized orbitals produces bandwidth changes in the electronic structure that move the system towards the metallic state, and so enhance conductivity (Raikh 1990). This same effect of orbital shrinkage and decreasing bandwidth has been seen to induce metal–insulator transitions in impurity bands (e.g. Hopkins *et al* 1989).

2.6. A word of caution

It is clear from this brief survey that various temperature and magnetic field dependencies are predicted for the conductivity of systems close to the metal–insulator transition. Fitting of data to verify or deduce precise functional forms is, however, seductively deceptive. Very accurate data covering wide temperature and resistance ranges are required, and, even then, apparently good fits can be erroneous if the system is in a transition region, or if more than one process is active, or if there are even small levels of sample inhomogeneity. The presence of such complications is not necessarily shown by the error analyses of fitting programmes. Furthermore, the theoretical treatments of models are themselves only approximate in that they often involve extrapolation of processes from regions far from the transition, where they are well supported, into the region of the transition itself where they are not. Our analyses should therefore be viewed as attempts to deduce as much as possible, bearing in mind the approximations of theory, and the precision and limited range of our data.

3. Experimental details

The nine a-$Si_{1-y}Ni_y$:H samples were produced by radio-frequency sputtering from silicon targets on which various amounts of nickel had been placed. Corning 7059 glass substrates were used for their high resistivity. The substrates were at room temperature during deposition and the sputtering gas was a 90% Ar and 10% H_2 mixture. The hydrogen was added to saturate silicon dangling bonds that might be present as a result of the disorder.

Compositions of the samples were determined to an accuracy of about ±2% by energy-dispersive analysis with x-rays (EDAX). Film thicknesses, which were generally about 1 μm, were measured to ±0.1 μm using a Talysurf stylus, and results verified in some cases by optical interference techniques. Electron diffraction measurements in a transmission electron microscope demonstrated the amorphous nature of the material. Extended x-ray absorption fine structure (EXAFS) measurements basically confirmed this result, but there was some indication in early data on similar samples of clustering of the nickel (Edwards *et al* 1989). This is significant in relation to the interpretation of the hopping conductivity discussed in section 4.2.

For electrical measurements, the thin film samples were scribed to define a conducting channel with Hall and resistance sidebars. All resistance measurements were made four-terminally to eliminate problems from any contact resistance. However, simultaneous two-terminal measurements gave no evidence for significant resistance at the contacts, which were made with indium.

The resistivity measurements were obtained by two different methods. The six samples in the metallic and transition regimes (52%, 50%, 29%, 26%, 23% and 17% Ni) were measured using standard four-terminal AC techniques. However, the three most resistive samples (7%, 8% and 15% Ni) could only be measured using four-terminal DC techniques due to the fact that unavoidable circuit capacitance gave rise to very large out of phase signals when AC methods were used so that accurate measurements could not be made. A Keithley 602 electrometer was used as the DC current source and a Keithley 604 differential electrometer was used as a voltmeter to measure the four-terminal potential difference. Resistance values were checked to be independent of drive current to verify that there was no significant Joule heating of the samples at low temperatures.

For measurements of conductivity and magnetoresistance between room temperature and about 6 K, samples were mounted in a continuous-flow cryostat with the sample chamber between the poles of a conventional electromagnet. For lower temperatures, standard ^{4}He cryostats with superconducting magnets were used. The magnetic fields were applied normal to the planes of the films.

4. Conductivity results

The conductivity data are shown in figure 1 in the form of a double logarithmic plot. Shown in this way, activated conductivity gives plots of negative curvature and metallic conductivity plots of positive curvature. The two samples with the higher Ni concentration are clearly metallic and show little variation of conductivity over the whole temperature range. The 29% and 26% samples also appear to be metallic, but the 23% film is interesting in that the curvature is negative at intermediate temperatures but appears, on the basis of the lowest data point, to become positive

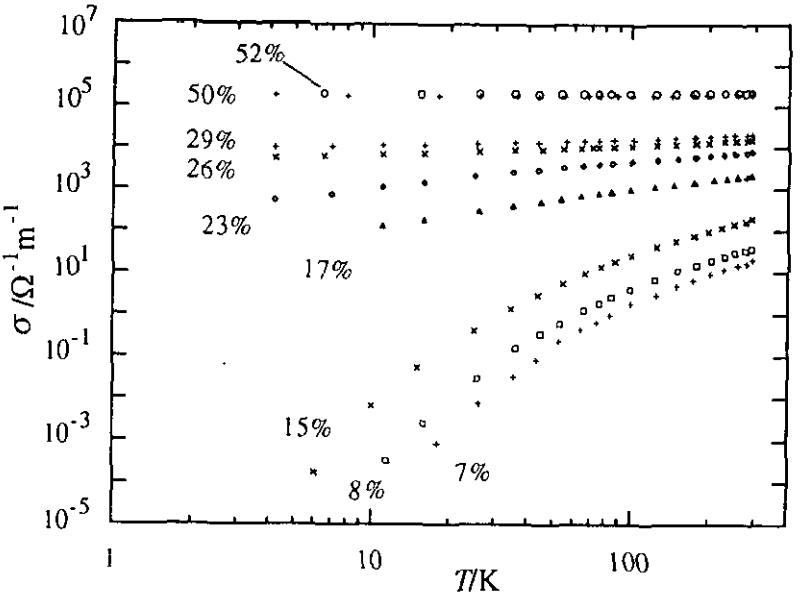

Figure 1. Conductivity as a function of temperature for all samples.

at lower temperatures. (This latter behaviour illustrates the importance of extending measurements to the lowest accessible temperatures.) The remaining samples appear to be well on the insulating side of the transition with the most resistive showing conductivity varying over six orders of magnitude.

4.1. The metallic and transition regimes

As explained in section 2, theoretical models suggest the presence of two temperature-dependent contributions to departures from Boltzmann conductivity, one from interaction effects and one from weak localization. The conductivity of metallic samples not too close to the transition is expected to obey equation (7):

$$\sigma = \sigma(0) + aT^{1/2} + bT^{p/2}. \tag{7}$$

Most results in the literature are fitted with $p = 2$ corresponding to inelastic scattering mediated by electron–electron interactions. The result of fitting one of our most metallic samples ($y = 0.50$) to this form is shown in figure 2, curve a. The solid curve is the fitted equation obtained by least-squares routines. The interaction term (a) comes out negative. Details are given in table 1, entry (a). It should be noted, however, that the square root term is strong and predicts a rapid change of gradient just at the lower end of the data range. There is no experimental evidence for this: the conductivity simply appears to become temperature-independent. This divergence of the fitted form from data at low temperatures is consistently present, even if more restricted temperature ranges of data are used. Furthermore, if lower-temperature data points are removed from the fitting calculations, the change in gradient of the calculated form moves to higher temperatures, keeping close to the lower data points included. This behaviour, produced by the negative $T^{1/2}$ term, is illustrated in

Table 1. Fitting of metallic and transition samples: The table shows the parameters obtained by least squares fitting to the form $\sigma = \sigma_0 + aT^x + bT^z$. Parameters set before fitting are shown in bold type.

Sample	$\sigma(0)/\Omega^{-1}$ m^{-1}	a/Ω^{-1} m^{-1} K^{-x}	x	b/Ω^{-1} m^{-1} K^{-y}	z	χ^2/Ω^{-2} m^{-2}	
50%	194 000	−420	**0.5**	64	**1**	50 000	a
	193 000	39	**0.5**	0.34	1.96	6300	b
	193 000	23	0.66	0.27	**2**	6400	c
	193 000	50	**0.5**	0.27	**2**	6400	d
29%	8000	800	**0.5**	−0.1	**2**	48 000	e
	7600	1000	**0.5**	−24	**1**	23 000	f
	6400	1900	**0.33**	−0.07	**1**	8000	g
	6400	1900	**0.33**	0.004	**2**	8000	h
	6000	2000	0.32	—	—	7800	i
	4500	3600	0.23	0.06	**2**	1300	j
	1700	6000	0.14	15	**1**	380	k
	2000	6000	0.15	6	1.2	360	l
26%	600	3400	0.24	0.001	**2**	8300	m
	500	3500	0.23	0.7	**1**	8300	n
	700	3300	0.24	—	—	8300	o
	2100	2100	**0.33**	−8.1	**1**	11 000	p
	2600	1800	**0.33**	—	—	55 000	q
23%	−400	360	0.76	−69	**1**	1700	r
	−700	500	0.53	−0.05	**2**	2100	s
	−1500	1000	0.39	—	—	7200	t

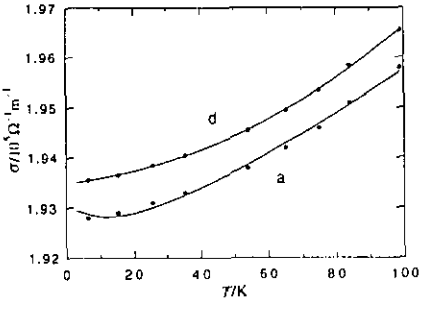

Figure 2. Data and theoretical fits for the 50% sample below 100 K. The curves show the least-squares best fits to the functional forms for inelastic scattering by (a) electron–electron scattering and (d) phonons. The invalidity of the former is apparent. (a and d refer to entries in table 1. Both the data and the fit for d are displaced vertically by 750 Ω^{-1} m^{-1} for clarity.)

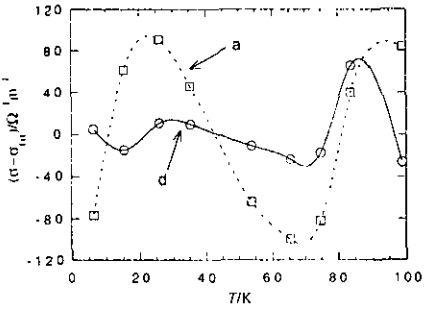

Figure 3. Differences between data and fitted forms for the 50% sample below 100 K. The forms used assume inelastic scattering by (a) electron–electron scattering, (d) phonons.

figure 3, curve a, which plots differences between measured conductivities and values calculated from the fitted equations.

These features of the calculated fits are strong evidence that the form being fitted is not valid. The procedure we have therefore generally used in exploring for the

best functional representation of our metallic and transition data, is to fit data for temperatures less than about 100 K to the form

$$\sigma = \sigma(0) + aT^x + bT^y \tag{9}$$

where the first of the temperature-dependent terms is allocated to interaction effects and the second to weak localization. Either or both indices can be set before fitting and some fits were also made with only one temperature-dependent term. Details are summarized in table 1. χ^2 provides a measure of the accuracy with which the fitted equations describes the data. It is defined by

$$\chi^2 = \sum_1^N (\sigma_i - \sigma(T_i))^2$$

where σ_i are the measured values and $\sigma(T_i)$ values calculated from the fitted equation. Clearly, minimum values of χ^2 correspond to the best fits. The restriction to data below 100 K is to ensure that low-temperature power-law forms (e.g. for phonon scattering) hold to reasonable accuracy.

Details of other fitting calculations applied to the 50% sample are given in rows b–d of the table. Parameters set before fitting are printed in bold typeface. We see that, when we set $x = 0.5$ before fitting, the routines give $z = 1.96$. Conversely, if we set $z = 2$, $x = 0.66$ is obtained. Despite the limited accuracy with which the parameters may be determined from our limited data set, the evidence is strongly in favour of the results being correctly described by $x = 0.5$ and $z = 2$. This is entry d in the table. The corresponding fit is shown in figure 2, curve d, displaced vertically by 750 Ω^{-1} m^{-1} for clarity, and differences between data and the fitted equation are shown in figure 3, d. This is clearly stable at low temperatures. We believe the structure evident in this fit at higher temperatures comes mainly from experimental error in the 84 K measurement. We conclude that the results for our most metallic samples are satisfactorily explained by a positive electron–electron interaction term with a weak-localization term mediated by inelastic electron–phonon scattering.

The 29% sample behaves very differently. Putting $x = 0.5$ and $z = 2$ gives a poor fit with a large value of χ^2. One might expect that close to the transition the dominant inelastic mechanism controlling the weak-localization contribution might become electron–electron scattering. However, putting $z = 1$ produces little improvement in χ^2 and also results in an apparent change of sign of the weak-localization term. Setting $x = 0.33$ in accordance with a predicted change in the interaction term (see section 2) produces some improvements with both $z = 2$ and $z = 1$ (g and h), but the weak-localization terms are small in both cases and the overall result is not very different from that obtained by including only one temperature-dependent term and determining its best index which comes out as $x = 0.32$ (i). Setting $z = 1$ or $z = 2$ and allowing x to vary produces much smaller values of x and the best fit is obtained with $z = 1$ and $x = 0.14$. This gives excellent agreement with the data as is shown by the very small value of χ^2. Starting with all parameters close to the values given by this fit, but now allowing both x and z to change produces the result shown in l. The only significant change is a suggestion of very slight strengthening of the temperature dependencies. There is no theoretical explanation for such small values of x as found in these fits.

As regards the behaviour of the 29% sample, we conclude that the variation of conductivity is primarily controlled by a positive interaction effect with a much

weakened temperature dependence together with a significant contribution from weak localization subject to inelastic scattering via electron–electron scattering.

The best fits for the 26% sample are obtained with $x \approx 0.24$ and it makes little difference whether the second temperature-dependent term is included with $z = 2$ or $z = 1$ (m–o). Much worse fits are obtained by putting $x = 0.33$ (p, q). It should also be noted that the best fits give small values of $\sigma(0)$. We conclude that this sample is close to the metal–insulator transition and that the temperature dependence of its conductivity is dominated by interaction effects, again with a weakened temperature dependence.

Attempts to fit the conductivity results of the 23% sample in a similar way immediately show that the basis of the analysis is invalid (r–t). In particular, all attempts at fitting produce a negative $\sigma(0)$, which is unphysical. One concludes on the basis of the range of data available in these experiments that this sample lies on the insulator side of the transition. Attempts to extrapolate conductivity data for the 23, 26 and 29% samples to zero temperature suggest that the transition lies in the region of 24–25% nickel. This is in agreement with estimates based on optical data (Davis *et al* 1989, Bayliss *et al* 1991).

4.2. The hopping regime†

As explained in section 2.5, activated conductivity in the insulating regime is normally interpreted in terms of variable-range hopping which gives the temperature dependence of equation (8):

$$\sigma = \sigma_0 \exp[-(T_0/T)^x] \tag{8}$$

in which, for three dimensional systems, $x = (p+1)/(p+4)$ where p is the power by which the density of states rises about the Fermi level as a function of energy. We used the following procedures to compare data to this equation.

(a) For a relationship of the above form, the logarithmic gradient is a linear function of the logarithm of the conductivity with gradient x:

$$\partial \ln \sigma / \partial \ln T = x(\ln \sigma_0 - \ln \sigma). \tag{10}$$

We therefore made cubic fits to the data of figure 1 and then calculated from them the required logarithmic gradient. Plots in the form of (10) then allowed us to identify ranges of conductivity and temperature over which (8) is obeyed. Corresponding straight line portions of the plots give the parameters x, T_0 and σ_0. This method is referred to as 'slope' in table 2. The method is useful but not robust as it imposes the cubic form on the data.

(b) We then carried out direct least-squares fitting to data identified by the above procedure as obeying (8), using the form $\ln \sigma = \ln \sigma_0 - (T_0/T)^x$ in order to give appropriate weighting to the measurements. We either allowed all parameters to vary or imposed $x = 0.5$ to obtain best corresponding values of σ_0 and T_0.

(c) In order to investigate the possible importance of any pre-exponential temperature dependence, we also carried out fitting to the form

$$\ln \sigma = AT^z \exp[-(T_0/T)^x]. \tag{11}$$

† Details of our analysis of the temperature dependence of the conductivity in the hopping regime have already been published (Abkemeier *et al* 1992). We include a brief account here for the sake of completeness.

Table 2. Fitting parameters for the hopping regime: the table shows the parameters obtained by least-squares fitting to equations (8) and (11). Parameters set before fitting are shown in bold type.

Sample	x	z	T_0/K	σ_0/Ω^{-1} m^{-1}	A/Ω^{-1} m^{-1} K^{-z}		Notes
7%	0.47	—	5000	860	—	Slope	All
	0.48	—	4000	700	—	Fit	All
	0.49	—	3500	500	—	Fit	$T < 200$ K
	0.50	—	3000	450	—	Fit	$T < 200$ K
	0.50	0.2	3000	—	200	Fit	All
8%	0.43	—	6000	1700	—	Slope	All
	0.44	—	5500	1400	—	Fit	All
	0.44	—	6000	1500	—	Fit	$T < 200$ K
	0.50	—	2500	550	—	Fit	$T < 200$ K
	0.50	0.4	2000	—	60	Fit	All
15%	0.45	—	3000	2600	—	Slope	$T < 100$ K
	0.42	—	5000	4500	—	Fit	All
	0.46	—	2500	2000	—	Fit	$T < 100$ K
	0.50	—	1500	1000	—	Fit	$T < 100$ K
	0.50	0.5	1100	—	70	Fit	All

The last of each group of entries in table 2 gives data for fitting to this form. Analyses according to (b) and (c) above are referred to as 'fit' in the table. The last column also gives the temperature range of the data used for the fitting calculations in the various cases.

Results of fitting calculations are summarized in the table where parameters whose values were fixed before fitting are shown in bold type. Fitting to (11) becomes ill-defined if all four parameters are allowed to vary (illustrating the difficulty of deducing detailed functional forms from experimental data). Values of z, even with constraints applied, are not well-defined but the implication of the fits to (11) with x set to 0.5 is that any pre-exponential temperature dependence has T to a low positive power. The 7% and 8% samples fit (8) well below 200 K. The 15% sample, closer to the transition, only fits well below 100 K. In all cases, $T_0 \gg T$, which is necessary for the analysis to be valid (Adkins 1989). Although determined values of x lie a little below 0.5, the evidence is very strong that the results are consistent with $x = 0.5$ which corresponds to variable-range hopping in a parabolic density of states: the behaviour predicted on the basis of the long-range Coulomb interaction model of Efros and Shklovskii (1975). Our results suggest that there is some increase of σ_0 as the transition is approached. Elefant *et al* (1991) found no change in σ_0 in their measurements on hopping conduction in a-$Ge_{1-y}Cr_y$. The full ranges of data for these three samples are shown plotted as $\ln\sigma$ against $1/T^{1/2}$ in figure 4.

In order to make detailed quantitative comparison with the Efros and Shklovskii theory, however, it is necessary to extract the coefficient g_2 of the implied density of states: $N(E) = g_2\epsilon^2$. The Efros and Shklovskii (ES) prediction, in the form given by Adkins (1989), is

$$g_2 = 2.02 \times 10^3(\epsilon_r\epsilon_0/e^2)^3 \tag{12}$$

a result depending only on the bulk relative permittivity ϵ_r. We shall make our quantitative comparisons for the 8% sample for which $\epsilon_r \approx 14$ (Bayliss *et al* 1991) a

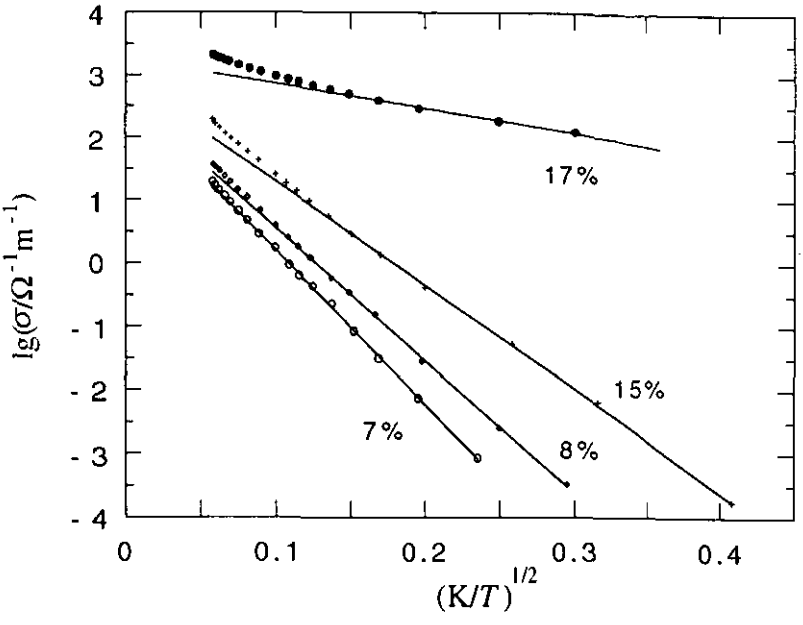

Figure 4. Conductivities of the four most activated samples plotted as $\lg \sigma$ against $1/T^{1/2}$. The lines are best linear fits to the low-temperature data.

value slightly enhanced above that of bulk silicon (11.9). This gives

$$g_{2es} = 2.3 \times 10^{86}\ \mathrm{J}^{-3}\ \mathrm{m}^{-3}.$$

Measured values of T_0, however, give a combination of g_2 and the tunnelling exponent α (Adkins 1989)

$$\alpha^3/g_2 = 2.7 \times 10^{-3}(kT_0)^3. \tag{13}$$

To separate these, another piece of information is required. We used the following approaches.

(i) We may estimate α for wavefunctions localized on the Ni atoms by using the Mott criterion for the metal–insulator transition: $n_c^{1/3}\alpha^{-1} \approx 0.26$ where n_c is the Ni concentration at the transition. This gives $\alpha \approx 8.7 \times 10^9\ \mathrm{m}^{-1}$. For an electron tunnelling further than the mean Ni–Ni distance (about 0.3 nm), the mean tunnelling exponent will be somewhat reduced. We take $\alpha_m \approx 8 \times 10^9\ \mathrm{m}^{-1}$. With (13), and taking $T_0 = 2500$ K (table 2) we obtain $g_2 = 4.6 \times 10^{90}\ \mathrm{J}^{-3}\ \mathrm{m}^{-3}$ which is more than four orders greater than the ES value. The value of α obtained in this way is therefore incompatible with an explanation for our data based on the ES model.

The optimum hop distance given by

$$R_{opt} = 0.25\alpha^{-1}(T_0/T)^{0.5} \tag{14}$$

also comes out unsatisfactory. At 10 K it is only 0.5 nm, rather less than two Ni–Ni distances. For variable-range hopping, it should be much larger than the inter-site

distance so that the tunnelling electron has a reasonably large number of final states to choose from. Similar problems arise in trying to fit the ES model to granular metal results (Adkins 1989).

(ii) If, alternatively, we assume the ES density of states to apply, we may calculate α from T_0. We then obtain very different results, namely $\alpha \approx 3 \times 10^8$ m^{-1} and $R_{opt} \approx 13$ nm at 10 K, about 40 Ni–Ni distances.

We thus obtain a consistent interpretation *if we assume that the wavefunctions of the mobile electrons are localized only over clusters of Ni atoms.* The localization volume now contains 10^3–10^4 Ni atoms, so the picture emerges of a relatively extended wavefunction, localized by longer-range disorder, and percolation is now clearly important.

It is relevant here that we attempted to estimate the correlation length by using the onset of non-ohmic conduction at 10 K to obtain a scale length over which the applied field provides energy changes modifying the electronic structure by amounts comparable to kT. We obtained $\xi \approx 25$ nm, about twice R_{opt} as calculated assuming the ES model to be valid. The similarity of these quantitities is satisfactory but raises important questions about the interpretation of normal variable-range hopping descriptions in systems near the metal–insulator transition for which correlation lengths become large. It is not clear what meaning could be attached to the idea of a hop that is shorter than the correlation length

Finally, it should be remarked that recent simulations have suggested that Coulomb interactions give rise to a single-particle density of states in three dimensions that rises about the Fermi level more rapidly than parabolically (e.g. Chicon *et al* 1988). If we accept the ES model as the explanation of our results, we can state that there is no evidence in our data for values of $x > 0.5$ which would be required by such 'hardening' of the Coulomb gap.

5. Magnetic measurements

5.1. The Hall effect

Attempts were made to measure the Hall effect in the more metallic samples. These were not successful because the small signals were noisy and obscured by components quadratic in the applied field. As a result, direct determinations of carrier concentration have not been possible in our work to date.

5.2. Magnetoresistance results

The two most metallic samples showed at 4.2 K a very small positive magnetoresistance, very close to the resolution limit of our electronics. In the interval 0–4 T, their resistances increased by about 0.1%. The analysis of the temperature dependence of the conductivity of the 50% sample indicated the presence of weak-localization and positive interaction contributions, but, over the temperature range analysed, the total change in conductivity they produce is very small, as would be expected far from the transition. Weak localization should contribute a negative magnetoresistance and interaction effects a positive. The implication of the figures in table 1 is that the conductivity at low temperatures is more influenced by weak localization, which is also as expected far from the transition. At 4 T the magnetic length L_B is 13 nm, which is probably many times greater that the mean free path,

so that it is likely that this field has relatively little effect on weak localization. We therefore conclude the the small positive magnetoresistance that is observed results from the effect of spin splitting on the electron–electron interaction terms.

The other magnetoresistance results are difficult to illustrate economically because of the wide variety of behaviour. At 1.7 K (figure 5) the magnetoresistance of the 23, 26 and 29% samples was positive at all fields, and the strength of the effect increased rapidly with reduction of nickel content. There was some suggestion of reduced gradient at low and high fields, but the general behaviour over the range of fields used was not far from linear. Unfortunately, the 17% sample was too resistive to measure at 1.7 K. In contrast, at 4.2 K (figure 6), the magnetoresistance increased with decreasing nickel content at first, reaching a maximum at about 26%, and then fell and became negative at low fields. The region of negative magnetoresistance, which was first present in the 23% sample and extended to about 1 T, strengthened and, by $y = 0.17$ extended to nearly 3 T. At the minimum, the resistance was decreased by nearly 4% in the 17% case.

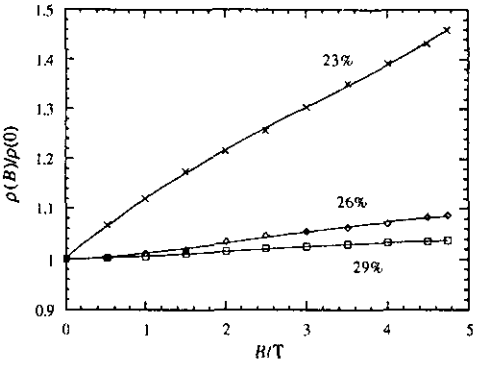

Figure 5. Magnetoresistance at 1.7 K.

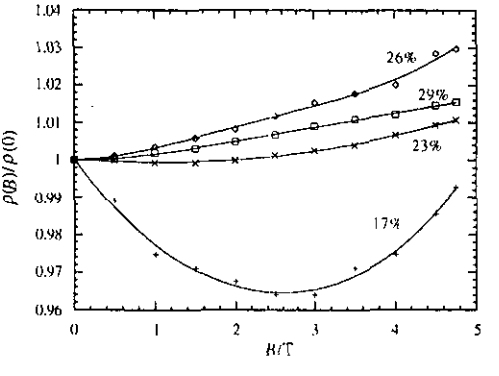

Figure 6. Magnetoresistance at 4.2 K.

We put forward the following explanations for these observations. In all cases, we attribute positive magnetoresistance to the effect of spin splitting on the electron–electron interaction contributions to resistance. As the transition is approached from the metal side, we expect electron–electron interactions to become stronger and more important relative to weak-localization effects. This is consistent with the increasing positive magnetoresistance as the nickel concentration is reduced. Also, for the applied field to be effective in modifying interaction effects, the temperature has to be sufficiently low that thermal energies are smaller than the field splitting. At 4 T, $\mu_B B/k = 2$ K, and this explains why the positive magnetoresistance increases rapidly with decreasing temperature in the interval between 4.2 K and 1.7 K. This temperature dependence also explains why it is only at 4.2 K that negative magnetoresistance is observed: in the range of our measurements it requires some suppression of magnetoresistance from interaction effects for the negative effect to become the larger.

The negative magnetoresistance we attribute to suppression of weak localization. In discussing the conductivity results, we argued that the transition in our system probably lies in the range $y = 0.24$–0.25. We first see negative magnetoresistance in

our 23% sample which is just on the insulator side of this range. As discussed in section 2.5, two explanations have been put forward for negative magnetoresistance in the localized regime, one based on weak-localization-type interference effects and the other on movement of the transition through changes in band structure caused by shrinkage of the localized orbitals by the field. We believe that one of these mechanisms is responsible for the negative magnetoresistance in the 23% and 17% samples. Since the negative magnetoresistance appears only at low fields in relation to the size of field required to produce significant orbital shrinkage (Yafet *et al* 1956), we believe that the weak-localization mechanism is responsible. Orbital shrinkage then explains the change to positive magnetoresistance at higher fields in the 17% sample.

We thus arrive at an interpretation of the magnetoresistance data which is totally consistent with that of the conductivity data.

6. Discussion

In the metallic regime, we have found best functional fits to our data with both weak-localization and electron–electron interaction contributions to the resistance. Far from the transition, the weak-localization contribution varies as T^2 indicating inelastic scattering by phonons, but, as the transition is approached, the temperature dependence weakens to linear as electron–electron scattering becomes more important. The electron–electron interaction contribution to conductivity is consistent with a $T^{1/2}$ behaviour far from the transition, but again the dependence on temperature weakens as the transition is approached becoming more like $T^{0.2}$. Throughout the ranges of temperature and composition studied, weak-localization and electron–electron interaction effects both give contributions causing the conductivity to increase with increasing temperature. Neither effect has anomalous sign.

The positive interaction contribution contrasts with behaviour found in recent studies of amorphous semiconductor–metal alloys where the metal is strongly magnetic. In a-$Si_{1-y}Cr_y$ (Möbius *et al* 1985) and in a-$Ge_{1-y}Cr_y$ (Elefant *et al* 1991) negative interaction terms were clearly present because well-defined conductivity minima were seen directly in the data. In a-$Ge_{1-y}Cr_y$ minima were observed in the range 15–50 K, the highest temperature minimum occurring in the most metallic sample studied. Albers and McLachlan (1991) also saw conductivity minima at some metal concentrations in a-$Ge_{1-y}Fe_y$. Early work in systems with non-magnetic metals cannot readily be compared with our results since the authors generally analysed their data in terms of a single temperature-dependent term. (Dodson *et al* 1981, Hertel *et al* 1983, Furubayashi *et al* 1985, Yoshizumi *et al* 1985.) We conclude that a negative interaction term in amorphous semiconductor–metal alloys appears to occur only when the metal is strongly magnetic.

Well in the activated regime, our system shows variable-range hopping with the temperature index $x \approx 0.5$, consistent with a parabolic density of states. This behaviour has been widely observed in similar systems: a-$Si_{1-y}Cr_y$ by Möbius *et al* (1983, 1985); a-$Si_{1-y}Au_y$ by Nishida *et al* (1982); a-$Ge_{1-y}Cr_y$ by Elefant *et al* (1991); a-$Ge_{1-y}Fe_y$ by Albers and McLachlan (1991) and by Massenet *et al* (1974); a-$Ge_{1-y}Au_y$ by Dodson *et al* (1981), the last two as reinterpreted by Möbius (1985). A few studies have been interpreted in terms of hopping in a constant density of states with $x = 0.25$: a-$Si_{1-y}Ni_y$:H by Rogachev *et al* (1987); a-$Si_{1-y}Au_y$ by McNeil

and Davis (1983); a-$Ge_{1-y}Mo_y$ by Yoshizumi *et al* (1985). Our quantitative analysis of the hopping regime, however, has shown that the results are consistent with the parabolic density of states originating in a Coulomb gap only if the localized states are relatively extended through networks of nickel atoms, the presence of which is to be expected statistically and for which there is some independent evidence in EXAFS studies (Edwards *et al* 1989). Such detailed quantitative analysis of hopping results has not been made by others working with semiconductor–metal alloy systems.

Our magnetoresistance measurements show regions of positive and of negative magnetoresistance. The positive magnetoresistance is attributed to spin splitting in the electron–electron interactions and becomes stronger as the transition is approached from the metallic side. The negative magnetoresistance was restricted to samples just on the insulating side of the transition at temperatures not too low so that there was some suppression of the positive contribution from interaction effects. The negative magnetoresistance was attributed to suppression of weak-localization-type interference (Nguyen *et al* 1985). The general pattern of behaviour we have found is similar to that seen in a-$Ge_{1-y}Mo_y$ by Yoshizumi *et al* (1988). Negative magnetoresistance in a-$Si_{1-y}Ni_y$:H in the hopping regime has also been observed by Rogachev *et al* (1987). Results in a-$Ge_{1-y}Fe_y$ reported by Albers and McLachlan (1991) also have some similarities to ours. Their samples with $0.24 > y > 0.16$ showed positive magnetoresistance at higher temperatures, changing to negative magnetoresistance at lower temperatures in a non-monotonic fashion that depended on both the metal content and the magnetic field. However, their most metallic samples all had negative magnetoresistance for $T < 4$ K, increasing as temperature was reduced, and their activated sample showed small *positive* magnetoresistance at *low* fields around 4 K but this became large and negative for high fields—the opposite of what we found. Tsugane *et al* (1981) also obtained negative magnetoresistance in an insulating sample of a-$Si_{1-y}Au_y$ at relatively high temperatures. The reversals from the behaviour seen by us can be attributed to spin–orbit scattering and/or the presence of a strongly magnetic atom. A maximum in magnetoresistance at the transition, as observed by us, was also seen by Ovadyahu and co-workers (Ovadyahu 1990) in two-dimensional In_2O_{3-x} films. However, their magnetoresistance was uniformly negative. They also demonstrated a sign reversal associated with spin–orbit scattering by adding small amounts of (the heavy metal) gold to their films.

The general constituents of magnetoresistance in amorphous systems near the metal–insulator transition now seem to be falling into place and our results fit the pattern that is emerging.

7. Summary

We have presented three dimensional conductivity and magnetoresistance results for a range of a-$Si_{1-y}Ni_y$:H alloys. In the metallic regime, we identify contributions to the conductivity from weak-localization and electron–electron interactions. Well in the metallic regime, the temperature dependence of the weak-localization contribution implies inelastic scattering by phonons, but nearer the transition electron–electron scattering becomes more important. The interaction contribution is of normal sign and shows weakened temperature-dependence near the transition.

Conductivity in the hopping regime is consistent with variable-range hopping in a parabolic density of states but detailed analysis shows that, if this is the result of a

Coulomb gap, then the localized states are extended over relatively large numbers of nickel atoms.

The magnetoresistance data show regions of both positive and negative magnetoresistance. Positive magnetoresistance, attributed to spin-splitting modification of the interaction effects, is found in metallic samples and in ones that are just on the insulator side of the transition at low temperatures and high fields. Negative magnetoresistance is only seen on the insulator side of the transition at not too low temperatures such that interaction contributions are somewhat suppressed.

The mechanisms we identify provide a consistent explanation of all our conductivity and magnetoresistance data that is in general accord with the current understanding of transport in disordered systems near the metal–insulator transition.

References

Abkemeier K M, Adkins C J, Asal R and Davis E A 1992 *Phil. Mag.* B **65** 675

Adkins C J 1989 *J. Phys.: Condens. Matter* **1** 1253

Albers A and McLachlan D S 1991 private communication

Altshuler B L and Aronov A G 1979 *Solid State Commun.* **30** 115

—— 1985 *Electronic Interactions in Disordered Systems* ed A L Efros and M Pollak (Amsterdam: North-Holland)

Bayliss S C, Asal R, Davis E A and West T 1991 *J. Phys.: Condens. Matter* **3** 793

Bergmann G 1983 *Phys. Rev.* B **28** 2914

—— 1984 *Phys. Rep.* **107** 1

Carl A, Dumpich G and Hallfarth D 1989 *Phys. Rev.* B **39** 3015

Chicon R, Ortu no M and Pollak M 1988 *Phys. Rev.* B **37** 10520

Davis E A, Bayliss S C, Asal R and Manssor M 1989 *J. Non-Cryst. Solids* **114** 465

Dodson B W, McMillan W L, Mochel J M and Dynes R C 1981 *Phys. Rev. Lett.* **46** 46

Edwards A M, Fairbanks M C, Newport R J, Gurman S J and Davis E A 1989 *J. Non-Cryst. Solids* **113** 41

Efros A L and Shklovskii B I 1975 *J. Phys. C: Solid State Phys.* **8** L49

Elefant D, Gladun C, Heinrich A, Schumann J and Vinzelberg H 1991 *Phil. Mag.* B **64** 49

Furubayashi T, Nishida N, Yamaguchi Y, Morigaki K and Ishimoto H 1985 *Solid State Commun.* **55** 513

Hertel G, Bishop D J, Spencer E G, Rowell J M and Dynes R C 1983 *Phys. Rev. Lett.* **50** 743

Hopkins P F, Burns M J, Rimberg A J and Westervelt R M 1989 *Phys. Rev.* B **39** 12708

Ioffe A F and Regel A R 1960 *Prog. Semicond.* **4** 237

Kawabata A 1980a *Solid State Commun.* **34** 431

—— 1980b *J. Phys. Soc. Japan* **49** 628

Lee P A and Ramakrishnan T V 1985 *Rev. Mod. Phys.* **57** 287

McNeil J and Davis E A 1983 *J. Non-Cryst. Sol.* **59 & 60** 145

Massenet O, Daver H and Geneste J 1974 *J. Physique Coll.* **35** C4 279

Möbius A 1985 *J. Phys. C: Solid State Phys.* **18** 4639

Möbius A, Elefant D, Heinrich A, Müller R, Schumann J, Vinzelberg H and Zies G 1983 *J. Phys. C: Solid State Phys.* **16** 6491

Möbius A, Vinzelberg H, Gladun C, Heinrich A, Elefant D, Schumann J and Zies G 1985 *J. Phys. C: Solid State Phys.* **18** 3337

Mott N F 1967 *Adv. Phys.* **16** 49

—— 1990 *Metal–Insulator Transitions* 2nd edn (London: Taylor and Francis)

Nguyen V L, Spivak B Z and Shklovskii B I 1985 *JETP Lett.* **41** 42

Nishida N, Yamaguchi M, Furubayashi T, Morigaki K, Ishimoto H and Ono K 1982 *Solid State Commun.* **44** 305

Ovadyahu Z 1990 *Hopping and Related Phenomena* ed H Fritzsche and M Pollak (Singapore: World Scientific)

Raikh M E 1990 *Solid State Commun.* **75** 935

Rogachev N A, Šmíd V, Mareš J J and Krištofik J 1987 *J. Non-Cryst. Solids* **97 & 98** 955

Shklovskii B I and Efros A L 1984 *Electronic Properties of Doped Semiconductors* (Berlin: Springer)

Tsugane S, Morigaki K and Nagashima C 1981 *Phys. Status Solidi* b **27** 3897
Yafet Y, Keyes R W and Adams E N 1956 *J. Phys. Chem. Solids* **1** 137
Yoshizumi S, Geballe T H, Kunchur M and McLean W L 1988 *Phys. Rev.* B **37** 7094
Yoshizumi S, Mael D, Geballe T H and Greene R L 1985 *Localization and Metal–Insulator Transitions* ed H Fritzsche and D Adler (New York: Plenum)